aqueous agar (1 M KCl), and above this, a saturated aqueous KCl solution in which the SCE was suspended. A simple one-compartment cell was used for voltammetry experiments. The working electrode was a glassy carbon disk set into a Teflon tube. Prior to a voltammetry experiment, the working electrode was polished with alumina paste on a micro polishing cloth (Buehler), by first using 0.30- and then 0.05-μm alumina (Buehler). The electrode was then sonocated in distilled water for 5 min and wiped dry. The electrode was installed into the voltammetry cell along with a platinum wire counter electrode and the reference. The solvent and electrolyte were then put into the cell and degassed with nitrogen. The working electrode was cycled many times between the anodic and cathodic limits of interest until there was no change in the charging current. The substrate was then introduced (1-5 mM), and the solution again was purged with nitrogen before the voltammetry experiment was initiated. Voltammograms were generally recorded at a sweep rate of 100 mV/s. After several voltammograms were obtained on the substrate in solution, a small amount of ferrocene was added, and the voltammogram was repeated, this time including the anodic couple of ferrocene along with the cathodic quinone couples. The $E°$ values of the quinone compound of interest were then determined placing the ferrocene couple at +0.47 V vs SCE.

Bulk Electrolysis. The bulk electrolyses of quinone compounds both in dilute solutions for spectroscopic analysis and in more concentrated solution for the preparation of solid samples were performed under similar constant potential conditions. A simple two-compartment cell was used, with a medium-porosity glass frit dividing the two chambers. For large-scale electrolysis, which usually required several hours, this glass frit was covered with a layer of the nonaqueous methylcellulose salt bridge material to hinder diffusion of substrate between the two chambers. The cell was then charged with solvent/supporting electrolyte (SSE). The auxiliary chamber was fitted with a carbon rod electrode. The working chamber was sealed with a flat Teflon cap through which the reference electrode and the glassy carbon voltammetry electrodes were suspended. Also suspended from the cap was a platinum wire, which held a large surface area carbon-felt electrode. This Teflon cap also provided a small hole through which a syringe needle introduced a flow of dry nitrogen through or above the solution. After a stir bar was placed into the working chamber, the Teflon cap was installed, and the solution was purged with nitrogen. The voltammetry electrode was used to measure a voltammogram on the blank SSE. The substrate was then introduced, and again voltammetry was used to check that the electrochemical response of the substrate was as expected. The BAS-100 used for voltammetry was disconnected from the cell, and a Princeton Applied Research (PAR) potentiostat Model 173 was connected to the cell. With good stirring in the working chamber, the carbon-felt synthesis electrode was stepped to the desired potential. A PAR-179 coulometer, connected to the potentiostat, measured the cathodic current passed. When 1-equiv of electrons had been passed, the current level had decreased to a very small value. At this point, the electrolysis was considered to be complete, and the resulting anion solution was sampled.

UV-Vis-Near-IR Absorbance Spectra. UV-vis-near-IR spectra were recorded with a Cary 14 spectrometer interfaced to an IBM compatible microcomputer. The computer interface allowed the subtraction of background absorbances and the storage of spectra on magnetic disks. Quartz cuvettes (Helma) of 1-cm and 0.1-cm path length were adapted for work in an inert atmosphere by the installation of a ground glass joint and a stopcock. Samples of anions from electrosynthesis were syringed into the argon-purged cuvette directly from the electrochemical cell, by use of a gas-tight syringe, and the spectrum was recorded immediately.

EPR Spectra. EPR spectra were recorded on a Varian E4 X-band spectrometer at room temperature. EPR samples were prepared in an inert atmosphere box under an argon atmosphere. A DMF solution of electrogenerated anion was diluted to the 1×10^{-5} M concentration range. The diluted solution was syringed into Pyrex tubes 8 in. in length and with an inner diameter of 1 mm. Several samples were prepared, including one from the concentrated solution. The tubes were sealed with small septa, removed from the dry box, and sealed with a torch. The EPR spectra were recorded within hours of sample preparation.

Infrared Spectra. IR spectra of anion radicals in DMSO solution were measured with a Perkin-Elmer 7100 FT-IR instrument. A 0.1 mm path length cell with calcium fluoride windows was used, because this material is resistant to DMSO solutions. Spectra were recorded in DMSO solution, 0.1 M in $LiClO_4$ and 5 mM in substrate, in the absence of oxygen. Background absorbances due to the DMSO solvent were subtracted from the spectra.

Acknowledgment. This work was supported by the National Science Foundation, the Office of Naval Research, SDI administered by the Naval Research Laboratory, and by the University of Minnesota Supercomputer Institute.

Systematic Study of a Series of Highly Fluorescent Rod-Shaped Donor-Acceptor Systems

R. M. Hermant, N. A. C. Bakker, T. Scherer, B. Krijnen, and J. W. Verhoeven*

Contribution from The Laboratory of Organic Chemistry, University of Amsterdam, Nieuwe Achtergracht 129, 1018 WS Amsterdam, The Netherlands. *Received June 5, 1989*

Abstract: The synthesis and emissive properties of bichromophoric molecules **1-11** are reported. All systems contain an anilino group as a one-electron donor (D) and various substituted ethylene moieties as electron acceptor (A) separated by a rod-shaped alicyclic framework provided by a piperidine ring. From the emissive properties it is concluded that in these molecules the electronic coupling between D and A is sufficient to allow complete charge transfer upon excitation (if thermodynamically feasible). The dipolar charge-transfer (CT) excited state thus populated displays a very strong fluorescence, which is highly solvatochromic (i.e., undergoes a large wavelength shift in response to changes of the solvent polarity), making these systems of interest as a new class of fluorescent probes. Variation of the acceptor group is found to allow design of such probes, with quantum yield vs solvent polarity profiles optimized for any particular polarity range.

1. Introduction

Recently we reported[1a] about the rod-shaped[1b] donor-acceptor systems **1** and **2** (see Figure 1), which show intense charge-transfer (CT) fluorescence in solution. In these molecules a dialkyl anilino moiety is acting as a one-electron donor (D) and a 1-vinyl-4-cyanonaphthyl (**1**) or a 2-vinylnaphthyl (**2**) moiety as a one-electron acceptor (A).

Neglecting the dipole moment in the ground state μ_0 relative to that of the excited (charge-transfer) state μ_e, Lippert[2] and Knibbe[3] derived relation 1. In equation 1, $\nu_{ct}(0)$ denotes the

$$\nu_{ct} = \nu_{ct}(0) - (2\mu_e^2/hc\rho^3)\Delta f \quad (1)$$

(1) (a) Mes, G. F.; de Jong, B.; van Ramesdonk, H. J.; Verhoeven, J. W.; Warman, J. M.; de Haas, M. P.; Horsman-van den Dool, L. E. W. *J. Am. Chem. Soc.* **1984**, *106*, 6524-6528. (b) The term "rodlike" was introduced by Zimmerman et al. to indicate extended bichromophoric systems. See: Zimmerman, H. E.; Goldman, T. D.; Hirzel, T. K.; Schmidt, S. P. *J. Org. Chem.* **1980**, *45*, 3933-3951.

(2) Lippert, E. *Z. Naturforsch.* **1955**, *10A*, 541-545.
(3) Beens, H.; Knibbe, H.; Weller, A. *J. Chem. Phys.* **1967**, *47*, 1183-1184.

0002-7863/90/1512-1214$02.50/0

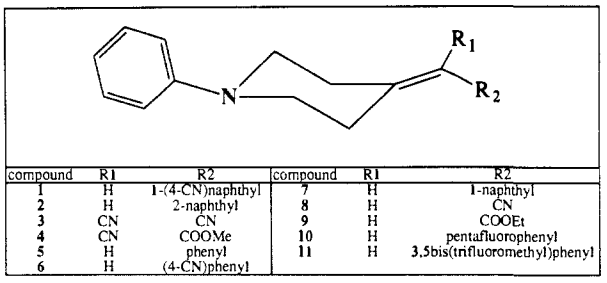

compound	R1	R2	compound	R1	R2
1	H	1-(4-CN)naphthyl	7	H	1-naphthyl
2	H	2-naphthyl	8	H	CN
3	CN	CN	9	H	COOEt
4	CN	COOMe	10	H	pentafluorophenyl
5	H	phenyl	11	H	3,5bis(trifluoromethyl)phenyl
6	H	(4-CN)phenyl			

Figure 1. Compounds studied.

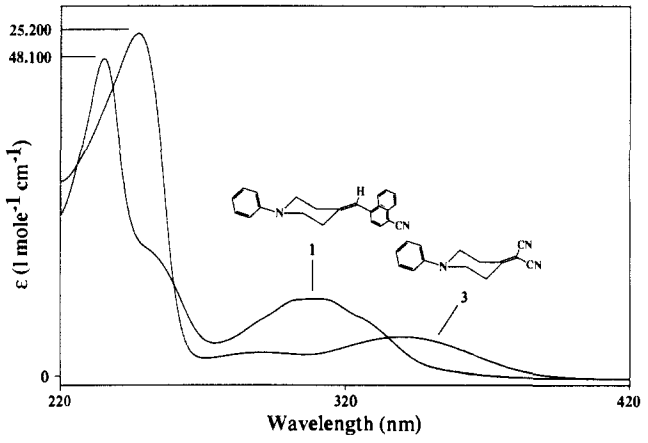

Figure 2. Electronic absorption spectra of compounds **1** and **3** in *n*-hexane.

wavenumber of the gas-phase CT fluorescence maximum and ρ the radius of a spherical cavity in which the molecule fits (Onsager model[4]). Δf represents a measure for solvent polarity defined by the dielectric constant ϵ and the optical refractive index n as $\Delta f = (\epsilon - 1)/(2\epsilon + 1) - (n^2 - 1)/(4n^2 + 2)$.

For an elongated shape of the molecule, ρ is usually estimated as 40% of its longest axis.[5] From the slopes of the plots of ν_{ct} versus Δf the dipole moments in the excited (charge-transfer) state were calculated as 28.4 D (**1**) and 28.9 D (**2**).[1]

The correctness of these huge values was checked via the time-resolved microwave conductivity (TRMC) technique developed by Warman and de Haas,[6] which gave a dipole moment of the relaxed S_1 states as 31 D (cyclohexane), 24 D (benzene), and 25 D (dioxane) for compound **1** and 21 D (cyclohexane) and 27 D (dioxane) for compound **2**. These values are in fair agreement with the dipole moments estimated from the fluorescence solvatochromism, although the TRMC-determined dipole moment for **2** in cyclohexane is rather small (see section 2.2.6).

By their unique combination of very strong solvatochromism and high quantum yield of the CT fluorescence, systems **1** and **2** appeared to point the way to a new class of fluorescent probes sensitive to the static as well as the dynamic polarization of the surrounding medium. In fact the latter property has already been exploited via an application of **1** as a very sensitive mobility probe in polymers.[7]

To investigate the influence of the acceptor–chromophore on the emissive properties and the application as a fluorescent probe, a series of compounds (**3–11**) has now been synthesized. The synthesis and photophysical properties of these new systems, together with those of **1** and **2**, are presented in this paper.

2. Results and Discussion

2.1. Electronic Absorption Spectra. Electronic absorption data of **1–11** in cyclohexane are compiled in Table I.

While these absorption spectra display negligible solvatochromism, an interesting aspect is formed by the appearance of

Table I. Electronic Absorption Data of Compounds **1–11** in *n*-Hexane[a]

1	2	3	4	5	6	7	8	9	10	11
234 (48 100)	249 (53 000)	248 (25 175)	250 (22 840)			227 (51 800)				
248 (19 700)	279 (14 000)	292 (1990)	292 (1990)	254 (24 400)	260 (27 000)	252 (16 700)	250 (13 300)	252 (13 700)	250 (20 100)	254 (24 000)
308 (11 700)	288 (sh, 13 800)	342 (2970)	338 (2170)	290 (sh, 3200)	290 (sh, 9600)	292 (10 100)	284 (3400)	290 (3300)	290 (sh, 3300)	290 (sh, 4500)

[a] Values are wavelength (nm) and, in parentheses, molar extinction coefficients (L/mol·cm).

Table II. Fluorescence Data of Compounds **1–11** in Various Solvents[a]

solvent	Δf	1	2	3	4	5	6	7	8	9	10	11
n-hexane	0.092	24.6 (0.20)	28.2 (0.26)[b]	22.0 (0.19)	21.8 (0.05)	29.6 (0.05)[b]	26.3 (0.26)	27.3 (0.06)	27.7 (0.23)	27.0 (0.03)	25.6 (0.29)	26.5 (0.22)
cyclohexane	0.100	24.4 (0.21)	28.1 (0.28)[b]	22.0 (0.21)	21.7 (0.06)	29.8 (0.05)[b]	26.2 (0.27)	27.3 (0.06)	27.7 (0.29)	26.9 (0.03)	25.3 (0.37)	26.5 (0.26)
dibutyl ether	0.194	21.5 (0.85)	27.1 (0.50)	19.5 (0.12)	19.5 (0.07)	28.9 (0.05)	23.5 (0.62)	25.8 (0.19)	25.2 (0.33)	24.3 (0.11)	21.6 (0.50)	23.9 (0.55)
diisopropyl ether	0.237	20.4 (0.78)	26.0 (0.57)	18.9 (0.05)	18.9 (0.02)	27.4 (0.05)	22.6 (0.53)	25.1 (0.28)	24.5 (0.30)	23.6 (0.12)	20.5 (0.28)	23.2 (0.67)
diethyl ether	0.251	19.5 (0.58)	24.8 (0.69)	18.1 (0.01)	18.1 (0.01)	27.0 (0.09)	21.4 (0.43)	24.3 (0.46)	23.1 (0.06)	21.7 (0.04)	19.8 (0.05)	22.1 (0.33)
ethyl acetate	0.292	17.5 (0.19)	22.8 (0.59)	*c*	*c*	24.7 (0.28)	19.7 (0.27)	22.3 (0.85)	22.2 (0.23)	21.2 (0.17)	*c*	20.4 (0.25)
THF	0.308	17.5 (0.16)	22.8 (0.50)	*c*	*c*	24.9 (0.19)	19.9 (0.21)	22.4 (0.74)	22.5 (0.25)	21.7 (0.21)	*c*	20.4 (0.13)
dichloromethane	0.319	17.3 (0.21)	21.8 (0.47)	*c*	*c*	23.9 (0.21)	19.2 (0.24)	21.6 (0.68)	20.8 (0.14)	19.8 (0.04)	*c*	20.3 (0.24)
acetonitrile	0.393	14.4 (<0.01)	19.2 (0.23)	*c*	*c*	21.9 (0.29)	16.7 (0.01)	19.0 (0.28)	19.3 (0.01)	18.5 (<0.01)	*c*	17.8 (0.03)
slope		33.9	41.2	23.9	22.2	36.4	32.1	35.7	28.4	28.9	36.2	29.3
intercept		27.9	35.2	24.3	23.9	35.9	29.5	33.1	30.6	29.8	28.9	29.5
corr coeff		0.992	0.985	0.988	0.988	0.980	0.989	0.981	0.976	0.965	0.996	0.988

[a] $\nu_{ct} \times 10^{-3}$ cm^{-1} (Quantum Yield) Slopes ($2\mu^2/hc\rho^3 \times 10^{-3}$ cm^{-1}), intercepts ($\nu_0 \times 10^{-3}$ cm^{-1}), and correlation factors of the linear correlations obtained according to eq 1 (see text) are also compiled. [b] Local fluorescence (see section 2.2.6). [c] No fluorescence was observed.

(4) Onsager, L. *J. Am. Chem. Soc.* **1936**, *58*, 1486–1493.
(5) Lippert, E. *Z. Electrochem.* **1957**, *61*, 962–975.
(6) de Haas, M. P.; Warman, J. M. *Chem. Phys.* **1982**, *73*, 35–53.
(7) van Ramesdonk, H. J.; Vos, M.; Verhoeven, J. W.; Möhlmann, G. R.; Tissink, N. A.; Meesen, A. W. *Polymer* **1987**, *28*, 951–956.

Table III. Estimated ρ Values (Å) and Excited-State Dipole Moments μ (Debye) of Compounds 1–11

	1	2	3	4	5	6	7	8	9	10	11
ρ	6.7	7.0	5.3	6.0	6.4	6.7	6.7	5.3	6.4	6.5	6.7
μ	31.8	37.5	18.8	21.8	30.8	31.0	31.9	20.5	27.4	31.4	29.6

a distinct long-wavelength transition in some of them (i.e., **3** and **4**) not attributable to the separate chromophores. This situation is exemplified in Figure 2, which shows the spectra of **1** and **3**. While in **1** the long-wavelength absorption is dominated by that of the vinylcyanonaphthalene chromophore, **3** displays a "new" band at 342 nm, which we attribute to an *intra*molecular CT transition. It is well documented that in a series of related D/A systems a direct correlation should exist between the position of the CT absorption and the difference between the redox potentials of D and A. Thus, from the difference between the reduction potentials of the acceptors incorporated in **1** and **3** (0.27 V; see Table IV), we predict that CT absorption for **1**, if any, should be located around 318 nm (based on the CT absorption in **3**). As evident from Figure 2, any CT absorption for **1** is probably obscured by the strong absorption of the acceptor chromophore in this region, although a distinct broadening of that absorption may indicate the presence of an underlying transition![1]

The large difference between the absorption spectra of compounds **2** and **7**, differing only in the positional attachment of the naphthalene moiety, is completely accounted for by the absorption characteristics of 1- and 2-vinylnaphthalene.[8] Thus, in most compounds **1–11** (except **3** and **4**) the absorption spectrum is dominated by that of the separate chromophores. In other papers[9] we will pursue in more detail the conformational and structural dependence of intramolecular CT absorption in **3**, **4**, and related systems.

2.2. Electronic Emission Spectra. As shown in the previous section, the absorption spectra of most of the systems studied closely resemble a superposition of those of the separate chromophores. The electronic emission spectra, however, are in general (see section 2.2.6) devoid of any emission typical for either of the chromophores. Instead a broad, red-shifted, and highly solvatochromic fluorescence, which is typical for emission from an intramolecular exciplex or charge-transfer state, is observed (see Figure 3). Since only charge-transfer emission is observed and since the excitation spectrum of this emission matches the absorption spectrum of the molecules, it may be concluded that, *irrespective* of the excitation energy, quantitative charge separation occurs. The interconnecting piperidine ring apparently acts as a very efficient electron-conducting chain, which is attributed to the occurrence of through-bond interaction (TBI) of the π chromophores via the σ system of the piperidine moiety. Such TBI was theoretically predicted by R. Hoffmann et al.[10,11] and further verified by many other theoretical and experimental studies.[12-15] The present results show that TBI can lead not only to rapid intramolecular electron transfer, but also to sufficient electronic coupling to allow for strong "exciplex-type" emission

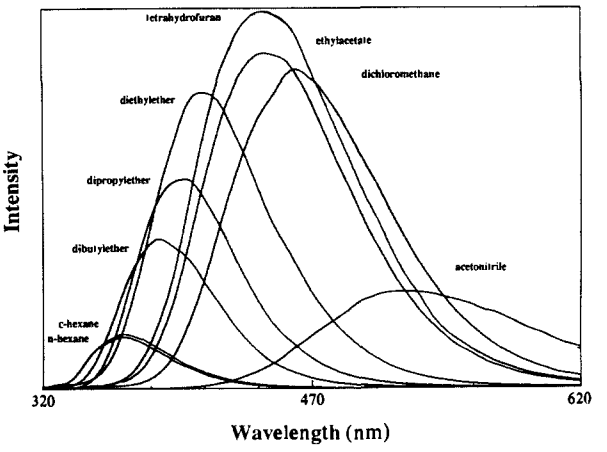

Figure 3. Typical solvatochromic CT emission of compound **7** in a series of solvents.

even in the absence of significant direct contact between the chromophores.

2.2.1. Influence of the Acceptor Chromophore on the Solvatochromism of the Fluorescence. In Table II the frequencies and quantum yields of the fluorescence of systems **1–11** in various solvents are compiled. Values for the slope ($2\mu^2/hc\rho^3$) and intercept (ν_0) of the regression lines obtained upon plotting ν_{ct} versus Δf (see eq 1) are also given in Table II together with the correlation coefficients of this regression. In order to compare more quantitatively the solvatochromic sensitivities of **1–11**, we plotted the ν_{ct} values for each of these in a series of solvents versus $\nu_{ct}(\mathbf{1})$ in Figure 4. This procedure has the advantage of "correcting" for specific solvent effects not included in eq 1. Indeed, very good linear correlations are observed (see Figure 4), with slopes between 0.72 and 1.17, that provide an objective measure for the relative solvatochromic sensitivities. From this comparison the highest solvatochromic sensitivities are found to be displayed by **2** and **10**.

Comparison with Other Solvatochromic Probes. The solvatochromism of electronic transitions with CT character has been exploited extensively as a spectroscopic polarity probe.[16] Most widely employed for this purpose are the strongly solvatochromic CT-type absorptions of Reichardt's $E_T(30)$ probe (a pyridinium-*N*-phenol betaine)[17] and Kosower's *Z* probe [1-ethyl-4-(methoxycarbonyl)pyridinium iodide],[18] which show comparable solvatochromic sensitivities. Their CT absorption maxima (in kcal/mol) define the $E_T(30)$ and *Z* solvent polarity scales.

Figure 5 now plots the fluorescence maximum of **1** (in kcal/mol) on the $E_T(30)$ solvent polarity scale. From the slope of the regression line (1.94) it is evident that the solvatochromic sensitivity of **1** [as well as that of most of the other systems (**2–11**)] significantly surpasses that of the $E_T(30)$ probe. Also, the sensitivities of some recently reported systems with highly solvatochromic emission[19a,b] and that of the absorption of some novel azo merocyanine dyes[19c] are significantly smaller than that of most compounds **1–11**. Apparently a larger effective change in charge separation between the ground and excited state is achieved in **1–11** than in the other probes. This larger change can be un-

(8) Klemm, L. H.; Ziffer, H.; Spraque, J. W.; Hodes, W. *J. Org. Chem.* **1955**, *20*, 190–199.
(9) (a) Krijnen, B.; Beverloo, H. B.; Verhoeven, J. W. *Recl. Trav. Chim. Pays-Bas* **1987**, *106*, 135–136. (b) Krijnen, B.; Beverloo, B.; Verhoeven, J. W.; Reiss, C. A.; Goubitz, K.; Heijdenrijk, D. *J. Am. Chem. Soc.* **1989**, *111*, 4433–4440.
(10) Hoffmann, R.; Imamura, A.; Hehre, W. J. *J. Am. Chem. Soc.* **1968**, *90*, 1499–1509.
(11) Hoffmann, R. *Acc. Chem. Res.* **1971**, *4*, 1–9.
(12) (a) Verhoeven, J. W. *Recl. Trav. Chim. Pays-Bas* **1980**, *99*, 369–379. (b) Verhoeven, J. W.; Paddon-Row, M. N.; Hush, N. S.; Oevering, H.; Heppener, M. *Pure Appl. Chem.* **1986**, *58*, 1285–1290.
(13) (a) Pasman, P.; Verhoeven, J. W.; de Boer, Th. J. *Chem. Phys. Lett.* **1978**, *59*, 381–385. (b) Oevering, H.; Paddon-Row, M. N.; Heppener, M.; Oliver, A. M.; Cotsaris, E.; Verhoeven, J. W.; Hush, N. S. *J. Am. Chem. Soc.* **1987**, *109*, 3258–3269.
(14) (a) Paddon-Row, M. N. *Acc. Chem. Res.* **1982**, *15*, 245–251. (b) Paddon-Row, M. N.; Jordan, K. D. In *Molecular Structure and Energetics*; Liebman, J. F., Greenberg, A., Eds.; VCH Publishers: New York, 1989; Vol. 6, Chapter 3.
(15) Klingensmith, K. A.; Downing, J. W.; Miller, R. D.; Michl, J. *J. Am. Chem. Soc.* **1986**, *108*, 7438–7439.
(16) Reichardt, Chr. *Solvents and Solvent Effects in Organic Chemistry*, 2nd ed.; VCH Verlagsgesellschaft mbH: Weinheim, 1988; and references cited therein.
(17) Reichardt, Chr. *Angew. Chem.* **1965**, *77*, 30–40.
(18) Kosower, E. M. *J. Am. Chem. Soc.* **1958**, *80*, 3253–3260.
(19) (a) Eckert, C.; Heisel, F.; Miehe, J. A.; Lapouyade, R.; Ducasse, L. *Chem. Phys. Lett.* **1988**, *153*(4), 357–364. (b) Tseng, J. C.-C.; Huang, S.; Singer, L. A. *Chem. Phys. Lett.* **1988**, *153*(3), 401–405. (c) Buncel, E.; Rajagopal, S. *J. Org. Chem.* **1989**, *54*, 798–809.

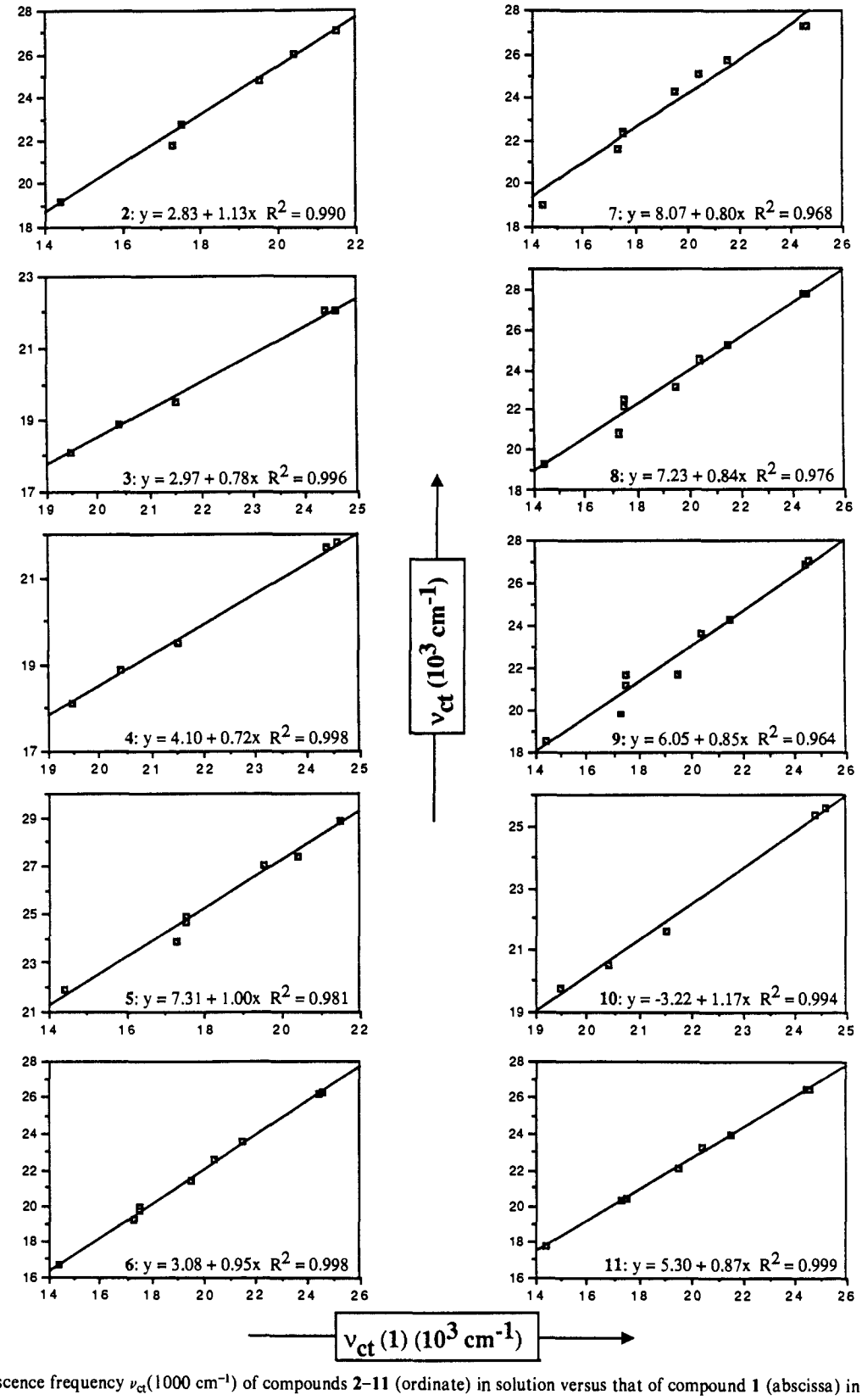

Figure 4. Fluorescence frequency ν_{ct}(1000 cm^{-1}) of compounds **2–11** (ordinate) in solution versus that of compound **1** (abscissa) in the same solvents.

derstood when it is realized that compounds **1–11** are assumed to be very apolar in the ground state while in the polar charge-transfer state the interconnecting piperidine ring keeps the oppositely charged chromophores at a long distance apart (vide infra).

In fact there are some cyanine dyes[20] the absorptions of which display even larger shifts than our probes, e.g., on going from acetone (λ_{max} = 641 nm) to water (λ_{max} = 472 nm). Unfortunately these dyes can only be used in a very limited polarity range and only in a mildly acidic environment.

2.2.2. Dipole Moments of 1–11 in the Excited State. Application of eq 1 allows an estimate of the excited-state dipole moment from the solvatochromism of the fluorescence, if a reasonable estimate of ρ can be made. For molecules that fit in an ellipsoidal cavity, ρ normally is estimated with a value equal to 40% of its long axis.[5] Although this procedure contains a certain degree of arbitrariness,[21] Table III compiles ρ values thus estimated for **1–11**

(20) Arai, S.; Yamazaki, M.; Nagakura, K.; Ishikawa, M.; Hida, M. *J. Chem. Soc., Chem. Commun.* **1983**, 1037–1038.

Table IV. Reduction Potentials (V ± 0.02) relative to Ag/AgCl (saturated KCl) in Acetonitrile of Compounds **1–11** As Measured by Cyclic Voltammetry[a]

	1	2	3	4	5	6	7	8	9	10	11
E_{red}	−1.76	−2.38	−1.49	−1.62	−2.70	−2.08	−2.33	−2.39	−2.32	−1.95[b]	−2.14

[a] Compounds **3–5** and **8–11** show an irreversible reduction wave. In analogy to the other compounds, $E_{1/2}$ is taken as the first cathodic peak potential plus 50 mV (scan speed 100 mV/s). [b] In this case the very weak first reduction wave was obscured by a more intense second one, resulting in a larger error of ca. 0.05 V.

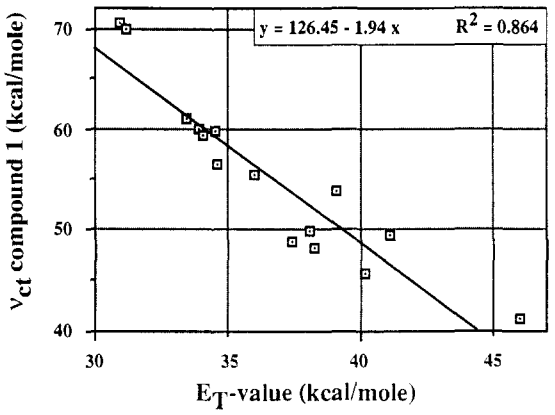

Figure 5. Fluorescence maximum of compound **1** (kcal/mol) in a series of solvents versus the $E_T(30)$ value of those solvents.

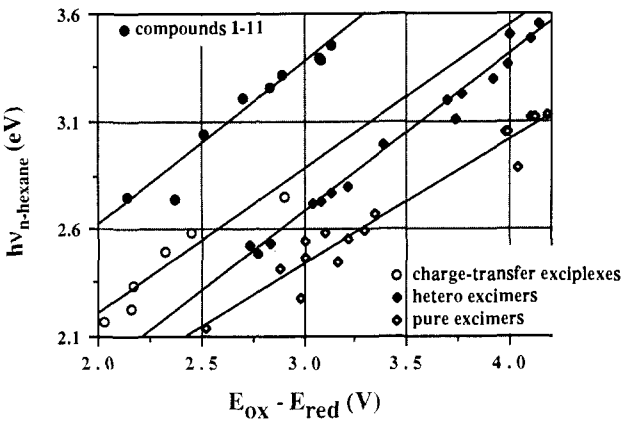

Figure 6. Fluorescence frequency of compounds **1–11** in *n*-hexane (in eV) together with those found for several intermolecular exciplexes and excimers, versus $E_{ox}(D)-E_{red}(A)$.

as well as the μ_e values derived by application of eq 1 to the $2\mu^2/hc\rho^3$ values listed in Table II.

The smallest μ_e value (18.8 D) is estimated for **3**, which still implies an effective charge-separation distance of 3.9 Å. This corresponds to the distance between the anilino nitrogen atom (donor) and the center of the acceptor double bond. The larger dipole moments in the other systems indicate increased delocalization of negative charge into the substituents at the double bond. The dipole moment in compound **2** (37.5 D) seems to be unexpectedly large. This is probably due to an overestimate of the effective ρ value because of the very elongated shape of this molecule.

Not withstanding such ambiguity in assigning the exact molecular shape of the emissive state, the magnitude of the μ_e values seems to warrant that the stretched ground-state conformation of these molecules, as shown for **1**,[1] **3**,[9b] **4**,[22] and **6**[22] by X-ray analysis supplemented by an ^{1}H NMR study of **1**,[1] is retained in the emissive state and that complete charge transfer from donor to acceptor occurs upon excitation.

2.2.3. Influence of the Acceptor Chromophore on the Fluorescence Frequency. Not only the solvent, but also the nature of the acceptor chromophore has a strong influence on the CT fluorescence. Theoretically[23] the energy level of a CT state, E_{ct}, relative to that of the ground state can be expressed by eq 2, where $E_{ox}(D)$ and $E_{red}(A)$ represent the one-electron oxidation and reduction potentials of donor and acceptor and C is a constant that depends on the degree of charge separation. Weller et al.[24]

$$E_{ct} = E_{ox}(D) - E_{red}(A) + C \qquad (2)$$

extensively studied the fluorescence of a large number of *intermolecular* exciplexes and excimers in *n*-hexane. Three separate classes were distinguished, which differ mainly in the extent of charge-transfer character: type I complexes or charge-transfer exciplexes with complete charge separation (dipole moments of ca. 14 D), type III complexes or pure excimers, evidently with no dipole moment, and type II complexes or mixed excimers with a character intermediate between type I and type III complexes.

For each of these classes a linear correlation between $h\nu_{ct}$ as measured in *n*-hexane and $E_{ox}(D) - E_{red}(A)$ was observed, where $E_{ox}(D)$ and $E_{red}(A)$ represent the electrochemical one-electron oxidation and reduction potentials of D(onor) and A(cceptor) as measured in acetonitrile solution (see Figure 6). As can be seen from Figure 6, the correlation lines are vertically displaced to higher energy with increasing dipole moment of the emitting state (I > II > III).

To compare our results with those found for the different intermolecular exciplexes, the reduction potentials of compounds **1–11** have been measured by cyclic voltammetry (see Table IV). It is assumed that the first detected reduction wave can be assigned to reduction of the acceptor–chromophore.

The correlation between $h\nu_{ct}$(*n*-hexane) and $E_{ox}(D) - E_{red}(A)$ for compounds **1–11** except **2** and **5**, is now also shown in Figure 6.

Once again a linear correlation is observed, but evidently it lies completely out of the range covered by intermolecular exciplexes. Thus, in *n*-hexane the position of the *intra*molecular CT fluorescence for **1–11** is shifted hypsochromically by a very significant amount (ca. 3700 cm^{-1}) with respect to the *inter*molecular type I exciplexes. This can be understood from a significantly larger intramolecular charge separation in the emissive state of **1–11** than in comparable intermolecular polar exciplexes. Larger charge separation destabilizes the excited state due to a decrease of its Coulomb stabilization given by $e^2/\epsilon r$ (r is the charge separation distance, e the elementary charge, and ϵ the dielectric constant of the solvent in question). For intermolecular exciplexes, $r = 3.2 \pm 0.2$ Å has been assumed.[25] This has to be increased to $r = 4.0 \pm 0.3$ Å to decrease the Coulomb energy by 3700 cm^{-1} in a medium with a dielectric constant of *n*-hexane (1.88). This corresponds well with the charge separation estimated above (see section 2.2.2) from the fluorescence solvatochromism of **1–11** and thus demonstrates the much larger spatial charge separation in **1–11** than can be achieved in the fluorescent state of intermolecular exciplexes that lack a rigid spacer to maintain such separation in competition with the Coulombic attraction.

2.2.4. Influence of Structure and Solvent on the CT Fluorescence Quantum Yield. Inspection of the data in Table II suggests that for each of the systems **1–11** a certain solvent polarity is required to evoke a maximum CT fluorescence quantum yield. Interestingly, variation of the solvent polarity allows one to evoke $\Phi >$ 25% for all systems carrying an aromatic moiety in the acceptor chromophore, while for the other systems (i.e., **3**, **4**, **8**, and **9**) the quantum yield remains relatively low over the whole range of

(21) Rettig, W. *J. Mol. Struct.* **1982**, *84*, 303–327.
(22) Unpublished X-ray data.
(23) Foster, R. In *Organic CT Complexes*; Academic Press: London, 1969.
(24) Weller, A. In *The Exciplex*; Academic Press Inc.: New York, 1975.
(25) Weller, A. *Z. Phys. Chem. Neue Folge* **1982**, *133*, 93–98.

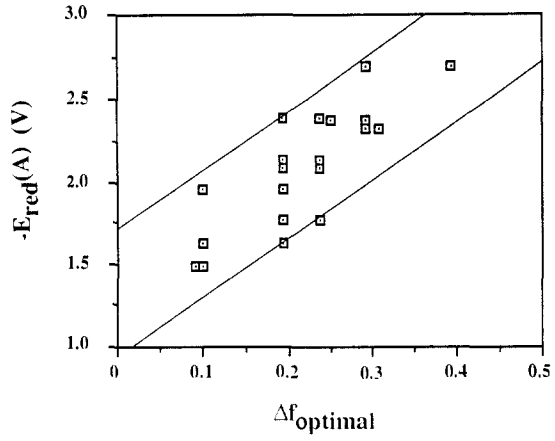

Figure 7. Solvent polarity Δf needed to evoke the two strongest emissions versus the one-electron reduction potential of the acceptor incorporated in **1–11**. The estimated boundaries of the correlation are also given.

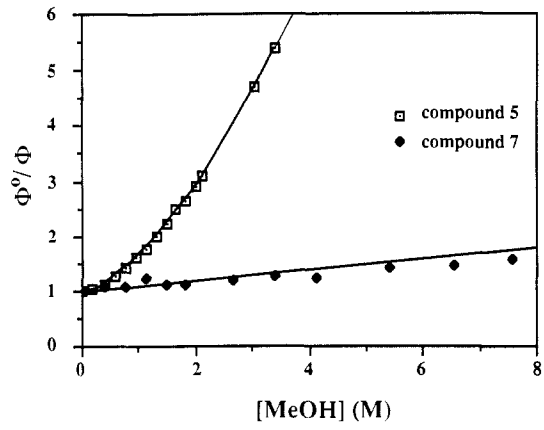

Figure 8. Stern–Volmer plot of the quenching of the CT fluorescence of compounds **5** and **7** in acetonitrile by methanol.

polarity studied (except **8**). We[26] commented earlier on the radiationless decay mechanism of D/A systems containing the acceptors incorporated in **3**, **4**, and **9**. It seems likely that a significant lowering of the torsional barrier to rotation around the exocyclic C=C bond in these acceptors upon electron attachment (i.e., in the CT excited state) leads to quenching of the CT fluorescence, since torsional motion around this bond can provide an efficient coupling of the CT excited state into nonradiative twisted excited (singlet and triplet) states of those acceptors. It is well documented[27] that aromatically substituted ethylenes are much less prone to radiationless decay via such twisting motions, thus rationalizing the higher fluorescence quantum yields of systems incorporating these aromatic acceptors.

From Table II it also can be seen that compounds **4** and **9**, containing a carbalkoxy group, show an absolute quantum yield of roughly 2–3 times lower than the corresponding cyano systems **3** and **8**, which have about the same reduction potential (see Table III). This might be due to the rotational freedom of the carbalkoxy group providing an additional dark process.

As is evident from Table II and illustrated in Figure 3, optimal Φ values can be evoked by variation of the solvent polarity. Interestingly, however, the polarity region in which relatively high quantum yields are obtained depends strongly upon the acceptor incorporated. Thus, with the weak acceptor incorporated in **5**, the most polar solvent probed (acetonitrile, $\Delta f = 0.393$) evokes intense emission while with the strong acceptor in **3** this occurs in a very apolar solvent (cyclohexane, $\Delta f = 0.100$). All other compounds display strong emission in a polarity range somewhere in between. Because of the interdependence between acceptor strength and fluorescence frequency, this implies (see also, Table II) that relatively strong emission always occurs within a frequency region between 20000 and 25000 cm^{-1}, suggesting that the energy gap between CT excited state and the ground state should have a value in the range between 2.48 and 3.10 eV in order to optimize the ratio between its radiative decay and competing dark processes. In order to make the interconnection between the polarity and the acceptor strength in respect to the maximum quantum yield more explicit, in Figure 7 we plotted the solvent polarity, Δf, needed to evoke the two strongest emissions versus the reduction potential of the acceptor–chromophore incorporated. From this figure it is clear that a correlation exists understriking the possibility to "tune" the fluorescing probe in such a way that a strong fluorescence can be achieved in any desired polarity range!

While it is well established that a small energy gap normally enhances direct radiationless interconversion to the ground state, the decrease of the fluorescence quantum yield at high values of the energy gap suggests increased crossover between the CT excited and other (locally) excited states. Because of the general absence of fluorescence from any of the separate chromophores, it appears likely that intersystem crossing to locally excited triplet states is involved.

2.2.5. Quenching of CT Fluorescence by Protic Solvents. It has been observed that the CT fluorescence of **1–11** is quenched in protic solvents like water and alcohols, which limits their applicability as a polarity probe in such solvents. In order to rule out solvent polarity as the source of this effect, the quenching of **5** and **7** in acetonitrile ($\Delta f = 0.393$) by methanol ($\Delta f = 0.393$) was measured.

During this quenching no change in fluorescence wavelength could be detected on addition of methanol, which is consistent with a lack of change in polarity. In Figure 8, Φ_0/Φ is plotted versus the concentration of methanol. From these Stern–Volmer plots K_{SV} values of 1.33 and 0.07 $L \cdot mol^{-1}$ are calculated. From the fluorescence lifetimes[28] of **5** and **7** in acetonitrile of 7.4 and 12.7 ns, respectively, k_q is calculated as 1.80×10^8 and 6×10^6 $L \cdot mol^{-1}\ s^{-1}$, respectively. In a comparable quenching experiment with water, K_{SV} values of ca. 1.0 and 0.1 $L \cdot mol^{-1}$, respectively were found, resulting in k_q values of ca. 1.35×10^8 and 8×10^6 $L \cdot mol^{-1}\ s^{-1}$. The diffusional rate constant in acetonitrile (2.3×10^{10} $L \cdot mol^{-1}\ s^{-1}$)[29] is at least a factor 100 (!) higher than these values. Thus, either a significant barrier exists for the quenching process and/or the quenching is coupled to ground-state complexation. The significantly different k_q values observed for **5** and **7** indicate that the quenching mechanism involves interaction of the protic solvent with the acceptor part and furthermore suggest that structural modification may allow the development of systems analogous to **1–11** that can also function as a polarity probe in protic solvents.

2.2.6. Thermodynamical Feasibility of Charge-Transfer Emission. For practically all compounds in all solvents probed, the relaxed CT state represents the lowest excited singlet state. In these cases, the complete absence of emission from primary populated locally excited states shows that electron transfer is very fast if the process is thermodynamically feasible (see section 2.2). The behavior of compounds **2** and **5** in apolar media deserves further comment.

For compound **2** in *n*-hexane and cyclohexane, a narrow, structured fluorescence band centered at ~28000 cm^{-1} ($\Phi = 0.28$) is observed (see Figure 9). In more polar solvents broad exciplex-type emission is observed, which shows the expected solvatochromism (see section 2.2.1). From these the extrapolated (via eq 1) CT fluorescence maximum of **2** in cyclohexane is calculated at 31700 cm^{-1}, which seems to put the CT state above locally excited states, preventing the CT state from acting as an emissive one or allowing concurrent emission from CT state and locally (acceptor) excited state. Upon protonation of compound **2** in

(26) Pasman, P.; Rob, F.; Verhoeven, J. W. *J. Am. Chem. Soc.* **1984**, *104*, 5127.

(27) (a) Bartocci, G.; Masetti, F.; Mazzucato, U.; Spalletti, A.; Baraldi, I.; Momicchioli, F. *J. Phys. Chem.* **1987**, *91*, 4733–4743, and references cited therein. (b) Karatsu, T.; Arai, T.; Sakuragi, H.; Tokumaru, K. *Chem. Phys. Lett.* **1985**, *115*(1), 9–15, and references cited therein.

(28) Hermant, R. M. et al., *to* be published.

(29) Martens, F. M.; Verhoeven, J. W. *Recl. Trav. Chim. Pays-Bas* **1981**, *100*, 228–236.

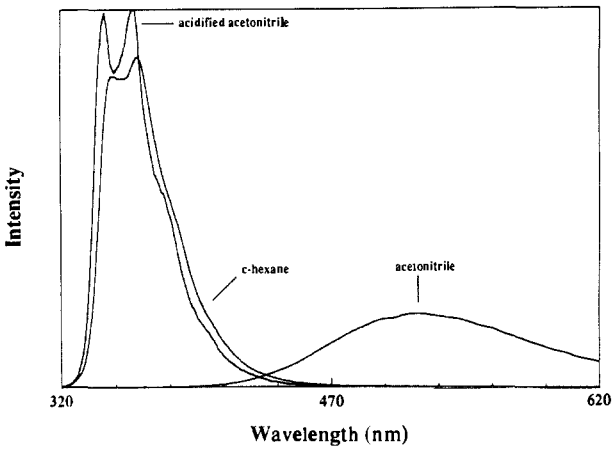

Figure 9. Emission of compound **2** in cyclohexane, acetonitrile, and acidified (HCl) acetonitrile.

acetonitrile its exclusive (CT) emission, centered at 19 200 cm^{-1} (Φ = 0.23), disappears completely, and instead, a narrow structured fluorescence, centered at 28 600 cm^{-1} (Φ = 0.34), is displayed (see Figure 9). This emission clearly stems from the vinylnaphthalene chromophore exclusively. Upon comparison with the latter (see Figure 9) the fluorescence of **2** in cyclohexane is found to be less structured, red-shifted, and also slightly less intense, indicating contribution of CT fluorescence. The occurrence of such "overlapping" dual fluorescence could account for the relatively small dipole moment (21 D) determined via the TRMC technique[6] and the reported observation of a biexponential fluorescence decay[1] in cyclohexane. More extensive time-resolved emission studies are in progress[28] to investigate the dual fluorescence in this type of donor–acceptor system.

Compound **5** in *n*-hexane and cyclohexane displays a narrow fluorescence band centered at 29 500 cm^{-1} (Φ = 0.04), which in structure and position is very similar to that reported for *N,N*-dimethylaniline.[30] Upon protonation of compound **5** in acetonitrile practically no fluorescence is observed, suggesting that the fluorescence of **5** in *n*-hexane and cyclohexane results from a locally excited anilino chromophore. In more polar solvents, again, broad solvatochromic emission is observed (see section 2.2.1) from which the extrapolated (via eq 1) CT fluorescence maximum in cyclohexane is calculated at 32 600 cm^{-1}, thus putting the relaxed CT state well above locally excited states. We thus assume that in apolar media compound **5** displays local fluorescence while in more polar solvents, in which charge transfer is thermodynamically feasible, CT fluorescence occurs exclusively. In conclusion, compounds **1–11** show CT fluorescence exclusively under conditions where the (relaxed) CT state represents the lowest excited state. Under these conditions electron transfer across the piperidine ring (which constitutes the internal conversion pathway from higher locally excited states to the CT state) is always fast.

3. Experimental Section

3.1. Syntheses. 1-Phenyl-4-piperidone was synthesized according to literature procedures.[31] After condensation of aniline (170 g, 1.83 mol) with 2 mol of methylacrylate in 70% yield, Dieckmann cyclization of the resulting diester was carried out in toluene with methanolate anion as a strong base. After extraction with 25% aqueous hydrochloric acid, the combined acidic water layers were boiled for 4 h. The cooled mixture was neutralized (pH 7) with concentrated aqueous NaOH and extracted with chloroform. After purification on a silica gel column and drying on $MgSO_4$, the reaction mixture was evaporated to give an orange oil [128.8 g; overall yield 40% (lit.[31] 25%)]. For spectroscopic purposes this was further purified by vacuum destillation to give an off-white solid: bp 110–120 °C (0.1–0.2 mmHg); mp 32–37 °C (lit.[31] mp 36–37 °C); IR ($CHCl_3$) 1710 (vs, CO), 1597 (vs, aryl), 1577 (m, aryl), 1495 (s, aryl) cm^{-1}; ^1H NMR (250 MHz, $CDCl_3$) δ 2.56 (t, 4 H), 3.62 (t, 4 H), 6.88–7.04 (td, 3 H), 7.35 (t, 2 H).

1-Phenyl-4-[(4-cyano-1-naphthyl)methylene]piperidine (1). The primary synthesis of this compound as, in more detail, described earlier,[1a] was carried out via Wittig condensation of triphenyl-(4-cyano-1-naphthyl)phosphonium bromide and 1-phenyl-4-piperidone with a yield of only 5%. We thus decided to carry out a synthesis by condensation of 1-phenyl-4-piperidone with diethyl (4-cyano-1-naphthyl)methylphosphonate (Wittig–Horner variant). Diethyl (4-cyano-1-naphthyl)-methylphosphonate was prepared[32] from triethyl phosphite and 4-(bromomethyl)-1-naphthonitrile.[33]

A solution of 0.53 g (3 mmol) of 1-phenyl-4-piperidone and 0.91 g (3 mmol) of diethyl (4-cyano-1-naphthyl)methylphosphonate in 10 mL of dry dimethoxyethane under a nitrogen atmosphere was cooled in ice. During 10 min 0.14 g of NaH (55–60% suspension in paraffinic oil) was added. the ice bath was removed and the reaction mixture was stirred for an additional 4 h. After addition of water and extraction with chloroform, the collected organic layers were dried on $MgSO_4$ and evaporated to dryness. The crude product was recrystallized from methanol to give yellow needles: yield 0.468 g, 48% (lit.[1] 5%); mp 121–122 °C (lit.[1] mp 124–125 °C); IR ($CHCl_3$) 2220 (m, CN), 1600 (s, aryl), 1580 (m, aryl), 1490 (s, aryl) cm^{-1}; ^1H NMR (250 MHz, $CDCl_3$) δ 2.4 (t, 2 H), 2.7 (t, 2 H), 3.2 (t, 2 H), 3.4 (t, 2 H), 6.7 (s, 1 H), 6.8–6.9 (td, 3 H), 7.1–8.3 (m, 8 H); high-resolution MS, found *m/z* 324.1627, calculated for $C_{23}H_{20}N_2$ 324.1626.

1-Phenyl-4-[(2-naphthyl)methylene]piperidine (2). The synthesis of this compound has been described[1a] previously.

1-Phenyl-4-(dicyanomethylene)piperidine (3). The synthesis of this compound has been described[9b] previously.

1-Phenyl-4-(cyanocarbomethoxymethylene)piperidine (4) was synthesized via Knoevenagel condensation, analogous to compound **3** on a 10-mmol scale in toluene, of methyl cyanoacetate (Merck) and 1-phenyl-4-piperidone. The crude product was recrystallized from ethanol to give yellow crystals: yield 1.22 g, 48%; mp 94–95 °C; IR ($CHCl_3$) 2220 (m, CN), 1725 (s, CO), 1592 (vs, aryl), 1490 (s, aryl) cm^{-1}; ^1H NMR (250 MHz, $CDCl_3$) δ 2.9 (t, 2 H), 3.2 (t, 2 H), 3.5 (tt, 4 H), 3.9 (s, 3 H), 6.84–6.92 (td, 3 H), 7.28 (t, 2 H); high-resolution MS, found *m/z* 256.1216, calculated for $C_{15}H_{16}N_2O_2$ *m/z* 256.1220. The structure was further confirmed by X-ray analysis.[22]

1-Phenyl-4-(phenylmethylene)piperidine (5) was synthesized on 3-mmol scale analogous to compound **1** from diethyl benzylphosphonate, which was prepared[32] on a 100-mmol scale from triethyl phosphite and benzyl bromide (Merck) (yield 100%). Purification on a silica gel column yielded a white solid: yield 0.078 g, 10%; mp 25–28 °C; IR ($CHCl_3$) 1594 (vs, aryl), 1572 (m, aryl), 1490 (vs, aryl) cm^{-1}; ^1H NMR (250 MHz, $CDCl_3$) δ 2.51 (t, 2 H), 2.64 (t, 2 H), 3.23 (t, 2 H), 3.34 (t, 2 H), 6.38 (s, 1 H), 6.83–6.95 (td, 3 H), 7.17–7.35 (m, 7 H); high-resolution MS, found *m/z* 249.1502, calculated for $C_{18}H_{19}N$ *m/z* 249.1518.

1-Phenyl-4-[(*p*-cyanophenyl)methylene]piperidine (6) was synthesized on a 3-mmol scale analogous to compound **1** from diethyl (4-cyanobenzyl)phosphonate, which was prepared[32] on a 25.5-mmol scale from triethyl phosphite and 1-bromo-4-tolunitrile (Aldrich) (yield 100%). The crude product was recrystallized from methanol to give nearly colorless crystals: yield 0.496 g, 60%; mp 102–103 °C; IR ($CHCl_3$) 2220 (vs, CN), 1594 (vs, aryl), 1490 (vs, aryl) cm^{-1}; ^1H NMR (250 MHz, $CDCl_3$) δ 2.52 (t, 2 H), 2.61 (t, 2 H), 3.24 (t, 2 H), 3.35 (t, 2 H), 6.35 (s, 1 H), 6.84–6.94 (td, 3 H), 7.22–7.62 (m, 6 H); high-resolution MS, found *m/z* 274.1426, calculated for $C_{19}H_{18}N_2$ *m/z* 274.1470. The structure was further confirmed by X-ray analysis.[22]

1-Phenyl-4-(1-naphthylmethylene)piperidine (7) was synthesized on a 3-mmol scale analogous to compound **1** from diethyl 1-naphthylmethylphosphonate, which was prepared[32] on a 231-mmol scale from triethyl phosphite and 1-bromomethylnaphthalene (yield 100%). The latter was synthesized on bromination of 1-methylnaphthalene with *N*-bromosuccinimide [yield 99.6% (lit.[34] 60%)]. The crude product of the final coupling reaction was recrystallized from methanol to give white crystals: yield 62 mg, 7%; mp 84–85 °C; IR ($CHCl_3$) 1594 (vs, aryl), 1572 (m, aryl), 1490 (vs, aryl) cm^{-1}; ^1H NMR (250 MHz, $CDCl_3$) δ 2.45 (t, 2 H), 2.66 (t, 2 H), 3.20 (t, 2 H), 3.44 (t, 2 H), 6.88 (s, 1 H), 6.85–6.97 (td, 3 H), 7.38–8.06 (m, 9 H); high-resolution MS, found *m/z* 299.1676, calculated for $C_{22}H_{21}N$ *m/z* 299.1674.

1-Phenyl-4-(cyanomethylene)piperidine (8) was synthesized on a 3-mmol scale analogous to compound **1** from diethyl cyanomethylphosphonate, which was prepared[32] on a 40.65-mmol scale from triethyl

(30) Berlman, I. B. In *Handbook of Fluorescence Spectra of Aromatic Molecules*; Academic Press: New York, 1971.
(31) Baty, J. D.; Jones, G.; Moore, C. *J. Chem. Soc. C* **1967**, 2645–2647.
(32) (a) Wadsworth, W. S., Jr.; Emmons, W. D. *J. Am. Chem. Soc.* **1961**, *83*, 1733–1738. (b) Bose, A. K.; Dahill, R. T. *J. Org. Chem.* **1965**, *30*, 505–509.
(33) McCullough, J. J.; MacInnis, W. L.; Lock, C. J. L.; Faggiani, R. *J. Am. Chem. Soc.* **1982**, *104*, 4644–4658.
(34) *Organikum*, 15th ed.; VEB Deutscher Verlag der Wissenschaften: Berlin, 1976; p 215.

phosphite and bromoacetonitrile (Aldrich). The crude product was recrystallized from methanol to give nearly colorless crystals: yield 0.48 g, 80%; mp 70–72 °C; IR ($CHCl_3$) 2217 (s, CN), 1594 (s, aryl), 1490 (s, aryl) cm^{-1}; ^1H NMR (250 MHz, $CDCl_3$) δ 2.5 (t, 2 H), 2.7 (t, 2 H), 3.4 (tt, 4 H), 5.2 (s, 1 H), 6.8–6.9 (td, 3 H), 7.3 (t, 2 H); high-resolution MS, found m/z 198.1146, calculated for $C_{13}H_{14}N_2$ m/z 198.1157.

1-Phenyl-4-(carboethoxymethylene)piperidine (9) was synthesized on a 3-mmol scale analogous to compound **1** from diethyl carbethoxymethylphosphonate, which was prepared[32] from triethyl phosphite and ethyl bromoacetate (Merck). Purification on a silica gel column yielded a pale yellow oil: yield 0.29 g, 40%; IR ($CHCl_3$) 1709 (vs, CO), 1600 (vs, aryl), 1579 (m, aryl), 1500 (s, aryl) cm^{-1}; ^1H NMR (250 MHz, $CDCl_3$) δ 1.3 (t, 3 H), 2.4 (t, 2 H), 3.1 (t, 2 H), 3.3 (tt, 4 H), 4.2 (q, 2 H), 5.7 (s, 1 H), 6.8–6.9 (td, 3 H), 7.3 (t, 2 H); high-resolution MS, found m/z 245.1400, calculated for $C_{15}H_{19}NO_2$ m/z 245.1416.

1-Phenyl-4-[(pentafluorophenyl)methylene]piperidine (10) was synthesized on a 1-mmol scale, analogous to compound **1** from diethyl (pentafluorobenzyl)phosphonate, which was prepared[32] on a 6.7-mmol scale from triethyl phosphite and pentafluorobenzyl bromide (Aldrich) (yield 83%). Because inferior NaH had been used, only partial reaction occurred. **10** was isolated from the reaction mixture by chromatography (silica gel/chloroform). Recrystallization from ethanol yielded colorless needles: yield 11.2 mg, 3.3%; mp 74–75 °C; IR ($CHCl_3$) 1594 (m, aryl), 1513 (m, aryl), 1489 (s, aryl), 1132 (m, aryl F) cm^{-1}; ^1H NMR (250 MHz, $CDCl_3$) δ 2.3 (br t, 2 H), 2.6 (t, 2 H), 3.3 (t, 2 H), 3.4 (t, 2 H), 5.9 (br s, 1 H), 6.8 (t, 1 H), 7.0 (d, 2 H), 7.3 (t, 2 H); high-resolution MS, found m/z 339.1048, calculated for $C_{18}H_{14}NF_5$ m/z 339.1046.

1-Phenyl-4-[[(3,5-bis(trifluoromethyl)phenyl]methylene]piperidine (11) was synthesized on a 3.08-mmol scale analogous to compound **1** from diethyl 3,5-bis(trifluoromethyl)benzyl phosphonate, which was prepared[32] on a 4.3-mmol scale from triethyl phosphite and 3,5-bis(trifluoromethyl)benzyl bromide (Aldrich) (yield 72%). Purification on a silica gel column yielded an off-white solid: yield 150 mg, 9%; mp 62–64 °C; IR ($CHCl_3$) 1593 (m, aryl), 1490 (m, aryl), 1277 (vs, CF_3) cm^{-1}; ^1H NMR (250 MHz, $CDCl_3$) δ 2.6 (m, 4 H), 3.3 (t, 2 H), 3.4 (t, 2 H), 6.4 (s, 1 H), 6.9 (t, 1 H), 7.0 (d, 2 H), 7.3 (m, 3 H), 7.65 (s, 1 H), 7.72 (s, 1 H); high-resolution MS, found m/z 385.1245, calculated for $C_{20}H_{17}NF_6$ m/z 385.1265.

3.2. Instrumentation. Electronic absorption spectra were recorded on a Hewlett-Packard 8451A diode array spectrophotometer and a Cary 17 D spectrophotometer.

Electronic emission and excitation spectra were recorded on a Spex Fluorolog 2 spectrophotometer.

Cyclic voltammograms were recorded with a Bank Electronic POS 73 Wenking potentioscan coupled to a HP 7090 A measurement plotting system. The reference electrode was Ag/AgCl, saturated KCl (−0.045 V vs SCE[35]), connected to an acetonitrile solution [electrolyte, tetraethylammonium tetrafluoroborate (0.1 M)] via a 3 M KCl salt bridge (E_{ox}(D) = 0.70 V vs SCE[36]).

(35) Bard, A. J.; Faulkner, L. R. In *Electrochemical Methods*; John Wiley and Sons: New York, 1980.

(36) Meites, L.; Zuman, P. In *Electrochemical Data*; John Wiley and Sons: New York, 1974; Part 1, Vol. A.

Infrared Spectroscopic Studies on the Photocatalytic Hydrogenation of Norbornadiene by Group 6 Metal Carbonyls. 1. The Role of H_2 and the Characterization of Nonclassical Dihydrogen Complexes, (η^4-Norbornadiene)$M(CO)_3(\eta^2$-H_2)

Sarah A. Jackson,[‡] P. Michael Hodges, Martyn Poliakoff,* James J. Turner, and Friedrich-Wilhelm Grevels[§]

Contribution from the Department of Chemistry, University of Nottingham, Nottingham, NG7 2RD England, and the Max Planck Institut für Strahlenchemie, D-4330 Mülheim a.d. Ruhr, Federal Republic of Germany. *Received June 19, 1989*

Abstract: This paper[1] describes the IR characterization of nonclassical H_2 complexes where ethene or norbornadiene (NBD) is coordinated to the *same* d^6 metal center as the η^2-H_2 and discusses the role of such complexes in the photocatalytic hydrogenation of NBD by group 6 metal carbonyl compounds. The dihydrogen complexes are generated in solution by the photolysis of alkene and diene carbonyl complexes in the presence of an overpressure of H_2 or D_2. Photolysis of *trans*-$(C_2H_4)_2M(CO)_4$ (M = Cr, Mo, and W) (**1**) in liquefied xenon (LXe) doped with H_2 or D_2 at −90 °C leads to the formation of *mer*-$(C_2H_4)_2M(CO)_3(H_2)$ (**2**) (with trans C_2H_4 groups) and *cis*-$(C_2H_4)M(CO)_4(H_2)$ (**3**). These species have been characterized by FTIR, and the ν(H–H) IR band of the coordinated η^2-H_2 has been detected for the W complexes. All of these compounds react thermally with N_2 to yield the corresponding dinitrogen complexes. Fast (microsecond) time-resolved IR (TRIR) is used to identify *fac*- and *mer*-(NBD)$M(CO)_3$(*n*-hept) as the primary photoproducts of the photolysis of (NBD)$M(CO)_4$ [M = Cr, Mo, and W] in *n*-heptane at room temperature. Detailed studies with Mo show that these intermediates react stereospecifically with N_2 and H_2 to give *fac*- and *mer*-(NBD)$Mo(CO)_3(X_2)$ (X_2 = N_2 and H_2). These species can also be generated in LXe by photolysis of either (NBD)$Mo(CO)_4$ or *mer*-(NBD)$Mo(CO)_3(C_2H_4)$. In addition, photolysis of (NBD)$M(CO)_4$ [M = Mo or W] in LXe yields products apparently containing η^2-NBD, which are not observed in the photolysis at room temperature, probably as a result of differences in temperature and photolysis sources. *fac*-(NBD)$Mo(CO)_3(H_2)$ appears to decay largely by loss of H_2, while *fac*-(NBD)$Cr(CO)_3(H_2)$ and *mer*-(NBD)$M(CO)_3(H_2)$ (M = Cr and Mo) do not decay by this pathway. A mechanism is proposed whereby transfer of H_2 to the diene in *mer*-(NBD)$M(CO)_3(H_2)$ leads to formation of norbornene (NBN) and in *fac*-(NBD)$M(CO)_3(H_2)$ leads to nortricyclene (NTC). The geometries of these two dihydrogen complexes provide a simple rationalization for the observed stereospecificity of the catalytic hydrogenation.

One of the prime examples of photocatalysis is the hydrogenation of dienes in the presence of group 6 transition metal carbonyls, $M(CO)_6$ (M = Cr, Mo, and W).[2a] The most striking feature of this hydrogenation is that, for conjugated dienes, hy-

‡ Present address: Laboratoire de Chimie Theorique, Universite de Paris Sud, 91405 Orsay Cedex, France.

§ Max Planck Institut für Strahlenchemie, Mülheim.

(1) Hodges, P. M.; Jackson, S. A.; Jacke, J.; Poliakoff, M.; Turner, J. J.; Grevels, F.-W. *J. Am. Chem. Soc.*, following paper in this issue.

0002-7863/90/1512-1221$02.50/0